OPTIMIZING THE MICROSTRUCTURE OF LOW-REM Nd-Fe-B SINTERED MAGNET USING $Tb_3Co_{0.6}Cu_{0.4}H_X$ ADDITION

Kateřina SKOTNICOVÁ [1], Gennady S.BURKHANOV [2], Tomáš ČEGAN [1], Natalia B. KOLCHUGINA [2], Alexander A. LUKIN [3], Ondřej ŽIVOTSKÝ [1], Pavel A.PROKOF'EV [2], Miroslav KURSA [1]

[1]*VSB-Technical University of Ostrava, Regional materials science and technology centre, Ostrava, Czech Republic, EU, katerina.skotnicova@vsb.cz*

[2]*Baikov Institute of Metallurgy and Materials Science, Russian Academy of Sciences, Moscow, Russian Federation*

[3]*JSC SPETSMAGNIT", Moscow, Russian Federation*

Abstract

Nd-Fe-B permanent magnets are key materials in the electric power system and they are indispensable for the future success of environmentally beneficial technologies. The hysteretic characteristics of sintered Nd-Fe-B magnets are highly sensitive to their microstructure and composition of phases. This paper is focused on the coercivity enhancement of the near-stoichiometric $Nd_2Fe_{14}B$-based magnet by optimizing microstructure, which included processes of grain boundary diffusion and grain boundary structuring via the application of hydrogenated $Tb_3Co_{0.6}Cu_{0.4}H_x$ compound added to the powder mixture. The base alloy having the composition Nd-24.0, Pr-6.5, Dy-0.5, B-1.0, Al-0.2, Fe-balance was prepared by strip-casting technique and subjected to hydrogen decrepitation during heating to 270 °C in a hydrogen flow at a pressure of 0.1 MPa and subsequent 1 h dwell at this temperature. The $Tb_3Co_{0.6}Cu_{0.4}$ alloy was prepared by arc melting of starting components in an argon atmosphere on a water-cooled copper bottom using a non-consumable tungsten electrode. The ingot was subjected to homogenizing annealing at 600 °C for 90 h and subsequent hydrogenation under the conditions used for the decrepitation of the strip-cast alloy. Hydrogenated $Tb_3Co_{0.6}Cu_{0.4}Hx$ compound and hydrogen-decrepitated strip-cast alloy were mixed and subjected to mechanical activation. The microstructure, phase composition and distributions of REM, Co, Cu for the prepared magnets were investigated by SEM/EDX method. It was found that the total REM content in the main magnetic $(Nd, Pr, Tb)_2Fe_{14}B$ phase was ~ 30 wt.%. Intergranular Nd-rich phases differing by their Tb, Co, Cu contents were identified. Studies of the stability of structure-sensitive parameter, namely, the coercive force ${}_jH_c$ of the sintered magnet prepared with 2 wt.% of $Tb_3Co_{0.6}Cu_{0.4}H_x$ addition to the low-temperature heat treatments show the increase in the coercive force up to 1480 kA/m. This phenomenon is not typical of sintered Nd-Fe-B magnets, which usually demonstrates the drop (or invariance) of the coercive force after low-temperature heat treatments at 350-450 °C.

Keywords: Nd-Fe-B magnets, strip casting, hydrides, heat treatment, coercivity

1. INTRODUCTION

Due to high values of the maximum energy product (BH_{max}), residual magnetic induction (B_r), coercive force in magnetic induction (${}_bH_c$), and coercive force in magnetization (${}_jH_c$) the Nd-Fe-B sintered magnets have found wide application in new energy fields, industrial motors, household appliances, and electronic information field. The obtainable maximum magnetic energy product has reached 471.9 kJ/m^3, which is approx. 93 % of the theoretical value (509 kJ/m^3) [1]. However, the highest coercivity of Nd-Fe-B sintered magnets obtained is approx. 2785 kA/m, less than 1/2 of the theoretical value (5809 kA/m) [2]. There is still much potential for increasing the coercivity of Nd-Fe-B sintered magnets, which are essential for powerful and space-saving

energy converters needed for the generation of electric power as well as for the conversion of electric to mechanic power (all kinds of electric motors). The increase in the characteristic $_jH_c$, which is associated with the temperature-time stability of sintered magnets, is achieved by alloying the base chemical composition ($Nd_{14-15}Fe_{bal}$ B_{6-8}) with elements such as Pr, Dy and Tb (the increase in the anisotropy field Ha); Ti, V, Mo and Nb (the prevention of grain growth during the sintering and structuring of the main magnetic phase 2-14-1); Al, Ga, Cu (the modification of the structure of boundary phases) as well as by using such technological processes as strip-casting, hydride dispersion, mechanical alloying, diffusion and saturation of the surface of the magnets with rare earth metals (Tb or Dy), followed by heat treatment at 1075-1175 K and multistage thermal treatment in the temperature range of 750-1275 K.

Nowadays, many research works have been made to simultaneously increase the coercive force and reduce the consumption of heavy rare-earth metals in the sintered Nd-Fe-B magnets. Alloying with Dy and/or Tb in the form of various compounds - oxides, fluorides, hydrides, intermetallic compounds and alloys resulted in certain successes. When using various additives in sintered Nd-Fe-B magnets, the mechanisms of grain boundary diffusion and grain boundary restructuring are realized. The use of binary mixtures makes it possible to improve the structure of the boundary phases and grain boundaries of the main magnetic phase and to realize the diffusion of the necessary alloy component directly across the boundaries. It was shown that by adjusting the time and temperature of the grain-boundary diffusion process, the coercivity of the magnet can be greatly increased without the significant loss of residual magnetization. The high cost of heavy rare earth metals and the limited availability of their resources all over the world determines the search for low-alloyed (by Tb, Dy, Pr, etc.) compositions and ways to save RE metals [3-9].

This paper is focused on the coercivity enhancement of the near-stoichiometric $Nd_2Fe_{14}B$-based magnet by optimizing its microstructure, which included processes of grain boundary diffusion and grain boundary structuring via the application of hydrogenated $Tb_3Co_{0.6}Cu_{0.4}H_x$ composition added to the powder mixture.

2. EXPERIMENTAL

The base alloy having the composition (wt.%) Nd-24.0, Pr-6.5, Dy-0.5, B-1.0, Al-0.2, Fe-balance was prepared by strip-casting technique and subjected to hydrogen decrepitation during heating to 270 °C in a hydrogen flow at a pressure of 0.1 MPa and subsequent 1 h dwell at this temperature. The $Tb_3Co_{0.6}Cu_{0.4}$ alloy was prepared by arc melting of starting components in an argon atmosphere on a water-cooled copper bottom using a nonconsumable tungsten electrode. This alloy was subjected to homogenizing annealing at 600 °C for 90 h (the analogous annealing conditions were used in [10]). After that, the alloy was subjected to hydrogenation in two modes: (mode 1) conditions applied for the strip-cast alloy, namely, heating to 270 °C in a hydrogen flow at a pressure of 0.1 MPa and subsequent 1 h dwell at this temperature, and (mode 2) stepped heating in hydrogen atmosphere and dwell at 200 °C and 500 °C in a glass Sieverts type apparatus were used. In the case of the stepped heating, the hydrogenation till obtaining the $Tb_3Co_{0.6}Cu_{0.4}H_x$ composition with x = 7.65 was realized. The hydrogenated $Tb_3Co_{0.6}Cu_{0.4}H_x$ compound and hydrogen-decrepitated strip-cast alloy were mixed and subjected to fine milling for 40 minutes till reaching average particle size of 3 μm using a vibratory mill and isopropyl alcohol medium. After wet compaction of the pulp in a transverse magnetic field of 1500 kA/m, blanks of magnets were sintered at T = 1080 °C for 2 h and subjected to an optimum heat treatment (HT) at 500 °C for 2 h. The following subsequent low-temperature stepped heat treatments were used (LTHT): 900 °C → 400 °C; 500 °C → 400 °C, 20 °C → (40 min) → 500 °C (20 min) → (6 h) → 400 °C (10 h). The high-resolution field emission gun-scanning electron microscope QUANTA 450 FEG equipped with an EDX APOLLO X microprobe was used for the investigation of microstructure and chemical composition of sample. Magnetic properties of the permanent magnet were measured using the automatic hysteresisgraph. The hydrogen and oxygen content was determined by ONH - 2000 ELTRA analyzer.

3. RESULTS AND DISCUSSION

3.1. SEM/EDX analysis

Chemical composition of the analyzed phases is summarized in **Table 1**, where the mean values obtained from three analyses are given for phases 1, 4 and 5. The microstructure of the sintered magnet prepared from the powder mixture with 2 wt.% of $Tb_3Co_{0.6}Cu_{0.4}H_x$ compound is shown in **Figure 1**. The stoichiometric composition of grains in the sample is close to that of the $Nd(R)_2Fe_{14}B$ phase (Phase 1 in **Figure 1**). The ideal Fe/R ratio (R = Tb, Pr, Dy) should be ~ 7. However, as it is seen from the calculation of the Fe/R ratio in **Table 1**, some differences take place. This is related to the existence of errors of determination of the phase composition, which are due to the closeness of the characteristic X-ray spectra of some elements. In particular, the excitation potential for the Lα - series of Dy is 6.494 keV, whereas for Fe, the excitation potential for Fe Kα is 6.403 keV. Therefore, the spectra with the lower intensity must be taken; this can give error in determining the quantitative phase composition of material. In this case for Dy, we used the Mα (1.293 keV) characteristic radiation for Dy. Another difficulty exists in determining the chemical composition for the area (since the electron beam diameter is ~ 2 μm). The several intergranular Nd-rich phases at triple junctions differing in the Co, Cu and REM were found (phase 2 in **Figure 1**). According to the data on the chemical analysis of Nd-rich phases in **Table 1**, the Tb content varied from 0 to 4 at.%, Dy content from 0 to 1.9 at.%, Pr content from 9.2 to 18.4 at.% and Nd content from 23.4 to 54.5 at.%. Other observed phases in the structure were REM-based oxides between grains of the sample (phase 3 in **Figure 1**). In accordance with literature data [11-12], these phases may correspond to NdO (the oxygen content is 50 at.%), Nd_2O_3 (the oxygen content is 60 at.%) or NdO_2 (the oxygen content is 67 at.%). The total oxygen content in the sample is approx. 5000 ppm. Nb-Fe-based compound is another observed phase, which is situated at the triple junction between the matrix grains (phase 4 in **Figure 1**). In addition to the main magnetically hard phase, the grains characterized by the increased Nd content and reduced Tb content are present in the magnet structure (phase 5 in **Figure 1**).

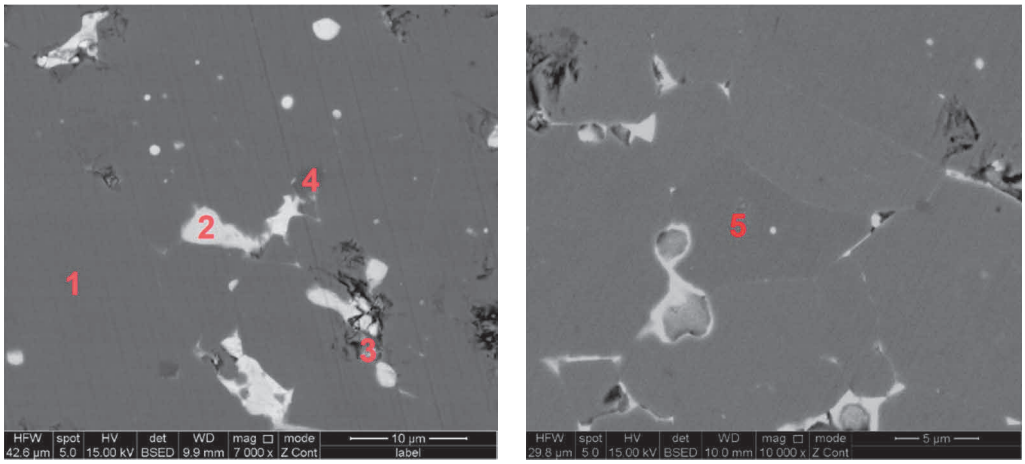

Figure 1 The microstructure of Nd-Fe-B sintered magnet prepared from the powder mixture with 2 wt.% of $Tb_3Co_{0.6}Cu_{0.4}H_x$ and marked analyzed phases

The low hydrogen content of 3 ppm (mean value) determined in the magnet by the method of inert gas fusion indicates the fact of the complete decomposition of $Tb_3Co_{0.6}Cu_{0.4}H_x$ compounds. The low nitrogen content of 36 ppm (mean value) denotes the absence of nitrogen penetration into the magnet material.

The distribution of rare earth elements, cobalt and copper in matrix grains and in the intergranular Nd-rich phases was studied using x-ray mapping. It is evident from **Figure 2** that Co, Cu, Nd and Pr distribution over the matrix grains is nearly homogeneous. Some Nd-rich phases contain a higher amount of Cu in comparison with other intergranular phases - see **Figure 2**.

Table 1 Chemical analysis of Nd-Fe-B sintered magnet prepared from the powder mixture with 2 wt.% of $Tb_3Co_{0.6}Cu_{0.4}H_x$

Area/phase	O_K	Tb_M	Dy_M	Al_K	Nb_L	Pr_L	Nd_L	Fe_K	Co_K	Cu_K
	(wt.%)									
Phase 1		2.1	1.2	0.3	0.2	5.8	21.5	67.6	0.9	0.4
Phase 2.1		0.0	0.0	0.4	0.2	24.6	50.7	9.4	4.1	10.7
Phase 2.2		1.5	1.3	0.9	0.2	15.7	40.4	39.2	0.8	0.0
Phase 2.3		1.4	1.0	1.1	0.2	15.3	39.8	39.8	0.9	0.6
Phase 2.4		5.3	2.5	0.0	0.1	19.3	62.9	8.4	0.9	0.6
Phase 3.1	11.6	4.5	2.4	0.0	0.1	17.5	56.0	6.8	0.8	0.3
Phase 3.2	13.1	5.2	2.4	0.0	0.1	17.8	57.6	2.7	0.9	0.4
Phase 3.3	20.1	4.5	2.2	0.0	0.1	17.0	52.6	2.4	0.8	0.3
Phase 4		0.2	0.2	0.0	58.6	0.4	1.5	38.4	0.4	0.3
Phase 5		1.1	1.0	0.3	0.5	6.1	22.2	67.1	1.1	0.7
	(at.%)									
Phase 1		0.9	0.5	0.7	0.2	2.8	10.2	83.2	1.0	0.4
Phase 2.1		0.0	0.0	1.6	0.2	18.4	37.1	17.7	7.3	17.7
Phase 2.2		0.8	0.7	2.7	0.2	9.6	24.2	60.5	1.2	0.0
Phase 2.3		0.8	0.5	3.4	0.2	9.2	23.4	60.5	1.4	0.8
Phase 2.4		4.1	0.0	0.2	0.2	17.1	54.6	18.8	1.8	1.2
Phase 3.1	51.0	2.0	1.0	0.1	0.1	8.7	27.3	8.5	0.9	0.3
Phase 3.2	56.1	2.2	1.0	0.0	0.0	8.6	27.3	3.2	1.1	0.4
Phase 3.3	68.1	1.5	0.7	0.0	0.0	6.5	19.7	2.4	0.7	0.3
Phase 4		0.1	0.1	0.1	46.8	0.2	0.8	51.0	0.6	0.4
Phase 5		0.5	0.4	0.8	0.3	3.0	10.6	82.5	1.3	0.7

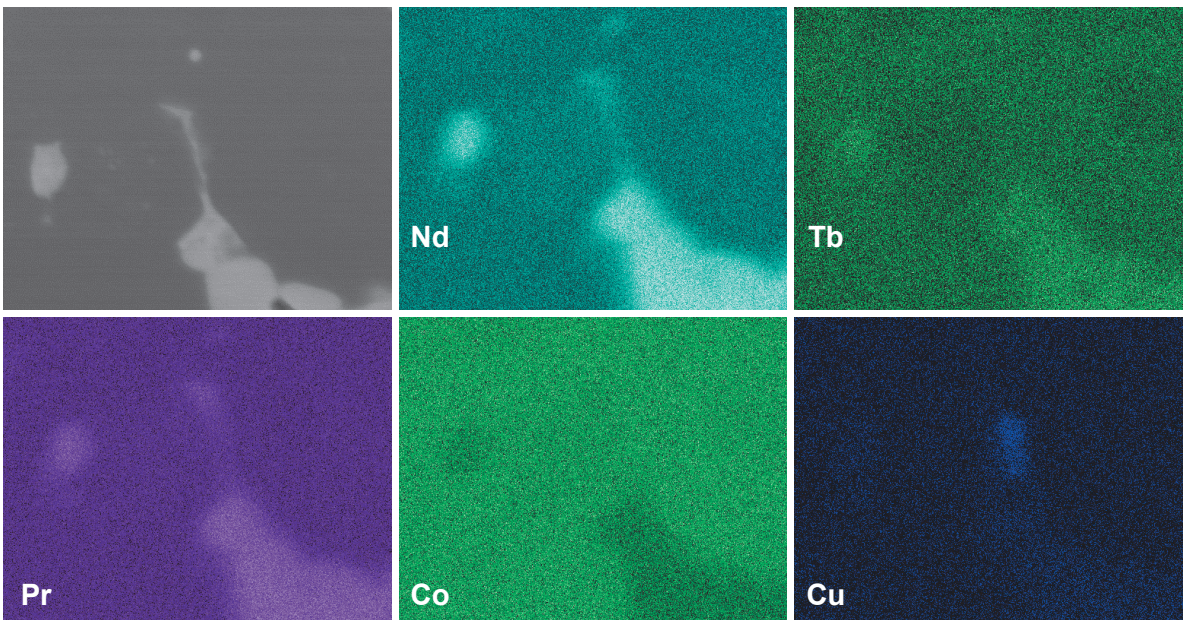

Figure 2 X-ray elemental mapping of REM, cobalt and copper in the matrix grains and Nd(R)-rich phases of Nd-Fe-B sintered magnet prepared from the powder mixture with 2 wt.% $Tb_3Co_{0.6}Cu_{0.4}H_x$

Figure 3 documents the line analysis through the grain boundaries at a step of ~1 μm. The results showed that some grains demonstrated characteristic inhomogeneous Tb distribution. The Tb content is high near the grain boundary (that is typical of the magnetic materials and magnets prepared by GBD techniques or from REM alloy-containing powders) and, as the distance from the grain boundary increases, it demonstrates wave-like variations. It should be emphasized that the higher terbium content corresponds to the lower neodymium (praseodymium) content.

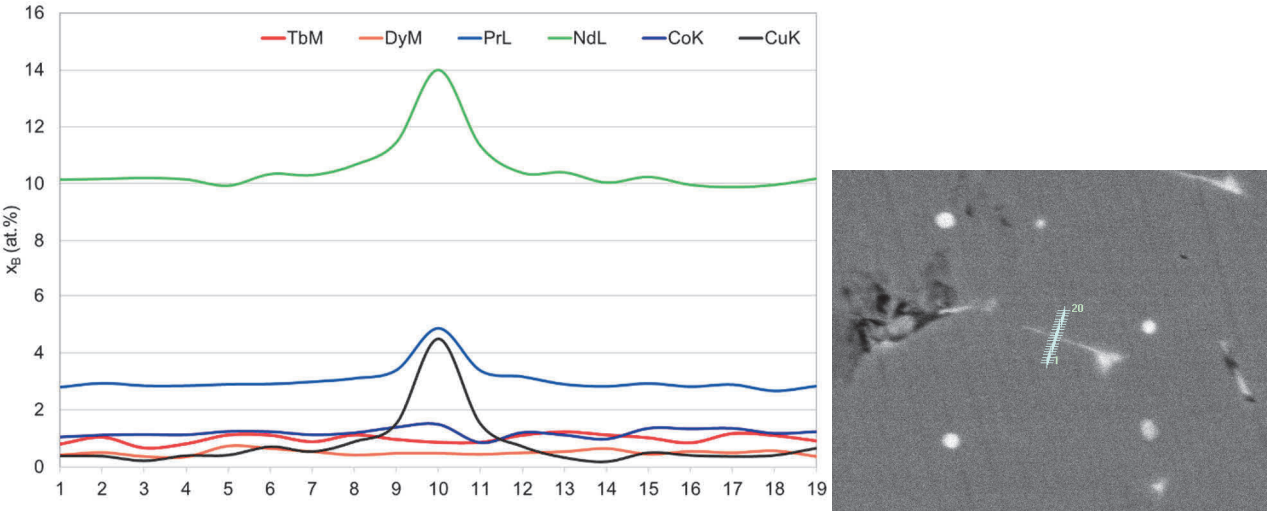

Figure 3 The line analysis through the grain boundaries in the Nd-Fe-B sintered magnet prepared from the powder mixture with 2 wt.% of $Tb_3Co_{0.6}Cu_{0.4}H_x$

3.2. Magnetic properties

Table 2 shows data on magnetic properties of sintered magnets prepared with 2 wt.% hydrogenated addition of $Tb_3Co_{0.6}Cu_{0.4}$, which are compared to those obtained for sintered magnets prepared with 2 wt.% of TbH_2 [3]. It should be noted that the magnetic properties of the magnets prepared with the hydrogenated $Tb_3Co_{0.6}Cu_{0.4}$ compound are higher than those in the case of TbH_2. One of the possible causes of the increase is the less oxidated state of additions in the case of the intermetallic compound. The other possible cause is the improved wettability of the $Nd_2Fe_{14}B$-phase grains with grain-boundary phases alloyed with cobalt and copper. Studies of the stability of structure-sensitive parameter of sintered magnets, namely, of the coercive force $_jH_c$ to the low-temperature heat treatments (annealing at temperatures below the optimum heat-treatment temperature (500 °C), are performed by estimating the time and temperature stability of magnets during their operation); they show the increase in the coercive force (**Table 2**) up to 1480 kA/m in the case of hydrogenated $Tb_3Co_{0.6}Cu_{0.4}$ addition. This fact is not typical for sintered Nd-Fe-B magnets, which usually demonstrate the drop (or constancy) of the coercive force after low-temperature heat treatments at 350-450 °C.

Table 2 Magnetic properties of Nd-Fe-B sintered magnet prepared from the powder mixture with 2 wt.% of $Tb_3Co_{0.6}Cu_{0.4}H_x$

Sample	B_r	$_jH_c$	H_k	$(BH)_{max}$
	(T)	(kA/m)	(kA/m)	kJ/m^3
Nd(Pr)-Fe-B + 2 % $Tb_3(Co_{0.6}Cu_{0.4})H_x$ + **optimum HT**	1.35	1336	1200	360
Nd(Pr)-Fe-B + 2 % $Tb_3(Co_{0.6}Cu_{0.4})H_x$ + **LTHT**	1.35	1480		

4. CONCLUSIONS

The performed structural and magnetic studies of sintered Nd-Fe-B magnet prepared from the strip-cast alloy show that the application of hydrogenated $Tb_3Co_{0.6}Cu_{0.4}H_x$ compound may efficiently enhance the coercivity of Nd-Fe-B magnets with slight sacrifice of their remanence. The increase in the hysteretic properties of magnet is related to the combined grain-boundary diffusion and grain-boundary restructuring effect realized during the special mode of heat treatment.

ACKNOWLEDGEMENTS

This paper was created within the project LTARF18031 "Development of physico-chemical and engineering foundations for the initiation of innovative resources-economy technology of high-power and high-coercivity (Nd,R)-Fe-B (R = Pr, Tb, Dy, Ho) low-REM permanent magnets" and within the project No. 14.616.21.0093 (the unique identification number RFMEFI61618X0093).

REFERENCES

[1] MITCHELL, I.V., COEY, J.M., GIVORD, D., HARRIS, I. R. and HANITSCH, R. *Concerted European Action on Magnets (CEAM)*. Essex: Elsevier Science Publishers LTD. 2012. 928 p.

[2] GUTFLEISCH, O., WILLARD, M.A., BRUCK, E., CHEN, C.H., SANKAR, S.G. and LIU, J.P. Magnetic materials and devices for the 21st century: Stronger, lighter, and more energy efficient. *Advanced Materials.* 2011. vol. 23, no. 7, pp. 821-842.

[3] LUKIN, A.A., KOLCHUGINA, N.B., BURKHANOV, G.S, KLYUEVA, N.E. and SKOTNICOVA, K. Role of terbium hydride additions in the formation of microstructure and magnetic properties of sintered Nd-Pr-Dy-Fe-B magnets. *Inorganic Materials: Applied Research.* 2013. vol. 4, no. 3, pp. 256-259.

[4] YUE, M., LIU, W.Q., ZHANG, D.T., JIAN, Z.G., CAO, A.L. and ZHANG, J.X. Tb nanoparticles doped Nd-Fe-B sintered permanent magnet with enhanced coercivity. *Applied Physics Letters.* 2009. vol. 94, 092501.

[5] GAOLIN, Y., MCGUINESS, P.J., FARR, J.P.G. and HARRIS I.R. Optimisation of the processing of Nd-Fe-B with dysprosium addition. *Journal of Alloys and Compounds.* 2010. vol. 491, pp. L20-L24.

[6] POPOV, A.G., VASILENKO, D.Yu., PUZANOVA, T.Z., SHITOV, A.V. and VLASYUGA, A.V. Effect of diffusion annealing on hysteretic properties of sintered Nd-Fe-B magnets. *The Physics of Metals and Metallography*. 2011. vol. 111, no. 5, pp. 471-478.

[7] LI, W.F., SEPEHRI-AMIN, H., OHKUBO, T., HASE, N. and HONO, K. Distribution of Dy in high-coercivity (Nd,Dy)-Fe-B sintered magnet. *Acta Materialia.* 2011. vol. 59, pp. 3061-3069.

[8] SEPEHRI-AMIN, H., UNE, Y., OHKUBO, T., HONO, K. and SAGAWA, M. Microstructure of fine-grained Nd-Fe-B sintered magnets with high coercivity. *Scripta Materialia.* 2011. vol. 65, pp. 396-399.

[9] LÖEWE, K., BROMBACHER, C., KATTERB M. and GUTFLEISCH, O. Temperature-dependent Dy diffusion processes in Nd Fe-B permanent magnets. *Acta Materialia.* 2015. vol. 83, pp. 248-255.

[10] BURKHANOV, G.S., LUKIN, A.A., KOLCHUGINA, N.B., KOSHKID'KO, Y.S., CWIK, J., SKOTNICOVÁ, K., ČEGAN, T., PROKOF'EV, P.A., DRULIS, H. and HACKEMER, A. Structure and phase composition of Tb3Co0.6Cu0.4 alloys for efficient additions to Nd-Fe-B sintered magnets. In *METAL 2017: 26st International Conference on Metallurgy and Materials*. Ostrava: TANGER, 2017. pp. 1775-1781.

[11] KIM, T-H., LEE, S-R., NAMKUMG, S. et al. A study on the Nd-rich phase evolution in the Nd-Fe-B sintered magnet and its mechanism during post-sintering annealing. *Journal of Alloys and Compounds.* 2012. vol. 537, pp. 261-268.

[12] WANG, S.C. and LI, Y. In situ TEM study of Nd-rich phase in NdFeB magnet. *Journal of Magnetism and Magnetic Materials.* 2005. vol. 285, pp. 177-182.